

CHERRY: Compressed Hierarchical Experts with Recurrent Representational Yield

*Selective token supervision, depth compression, and expert fusion
for compute-efficient language models*

Dohyeon Kwon¹

AX Architect

dh.kwon@teamsparta.co

First author

Youngjin Park, Ph.D.^{1,+}

Vice President

yj.park@teamsparta.co

† Corresponding author

AXOps Team, TeamSparta Inc., Seoul, South Korea

<https://ax.spartaclub.kr>

ABSTRACT

We study three complementary techniques for training compute-efficient language models and report the following findings.

(1) Selective supervision and per-token efficiency. Selective Ground Truth Token Training (SGT) concentrates supervision on the $\sim 15\%$ of output tokens that carry semantic payload. Through positive gradient coupling in position-shared transformer weights, a token-level instance of auxiliary-task transfer [44], the remaining 85% of unsupervised tokens still improve substantially. This yields a $4.5\times$ per-supervised-token efficiency: at the step-100 eval optimum, $\sim 67\%$ of the full-sequence loss reduction is recovered from 15% of the supervision. We prove that this improvement on unsupervised tokens is guaranteed whenever the gradient coupling coefficient $\bar{\gamma} = 0.72$ is positive (Theorem 3), and we show that the effect is a property of natural-language structure, collapsing on shuffled text (Corollary 5).

(2) Depth compression with recurrent recovery. A 48-layer, 1B-parameter transformer can be compressed to 6 layers (227M) by averaging adjacent layers and then restored through learned recurrent unrolling. With 34 effective recurrent layers, the 6-layer model reaches a held-out loss of 2.934, within measurement noise of a 566M dense model at 2.926, a $2.5\times$ reduction in parameters.

(3) Fusion of compressed experts. Assembling several compressed models as a Mixture of Efficient Experts (MoEE) with multi-token prediction improves over each single expert at comparable active parameters: a 2-expert MoEE reaches loss 2.789 versus 2.926 for the best single compressed model.

We validate these techniques on CHERRY-1.8B, a Korean foundation model whose every trainable parameter derives from our own training runs. We are explicit throughout about the scope of the evidence (one model family, Korean data, loss-based metrics) and about which claims are established versus prospective.

Keywords: wave propagation, selective training, depth compression, recurrent depth, mixture of experts, sovereign AI, foundation models

Preprint. June 2026.

1 Introduction

Building capable language models today requires substantial resources. DeepSeek-R1 [12] used thousands of GPUs to show that reinforcement learning alone can induce emergent reasoning. A.X-K1 [40] involved a large team to build a 519B-parameter Korean model, and GLM-5.2 [45] scales to 744B parameters. Scaling laws [17] suggest that frontier budgets are needed for frontier capabilities.

This paper explores a complementary direction: getting more out of a fixed budget. We study three techniques that, together, allow competitive models to be trained with substantially less compute.

The starting observation is that language-model supervision is often inefficient. In a typical instruction-response pair, only a minority of output tokens carry factual or reasoning content (cf. [26]); the rest is syntactic scaffolding that a pretrained model already produces well. Standard cross-entropy loss [36] weights all tokens equally, spreading the supervision signal across positions where it adds little.

We show that concentrating supervision on this semantic minority has three useful consequences.

1. A **gradient-coupling (“wave propagation”) effect** (Section 3.2): because transformer weights are shared across positions, a gradient step on the supervised tokens also improves the unsupervised ones. This is a token-level instance of auxiliary-task transfer [44]; we measure its magnitude and show it depends on linguistic coherence.
2. Selective supervision provides a signal strong enough to recover from **aggressive depth compression** (Section 3.3): 48 layers reduced to 6, with roughly 78% of the loss gap recovered in 500 steps.
3. Compressibility enables **expert fusion** (Section 3.4): several compressed models, assembled as mixture-of-experts [39] experts, improve over any single model at the same active-parameter budget.

We validate these techniques on CHERRY-1.8B (Section 5), a Korean foundation model whose every trainable parameter derives from our own training runs, with no dependence on any external model’s weights at inference time. We use *sovereign* in this specific, narrow sense throughout (Table 13).

Contributions..

- We characterise the wave-propagation effect as positive gradient coupling, prove that it guarantees improvement of unsupervised tokens when the coupling is positive (Theorem 3), and measure it on held-out data.
- We demonstrate depth compression with recurrent recovery ($2.5\times$ fewer parameters at loss within noise of the dense baseline).
- We introduce MoEE, a fusion of compressed experts with selective distillation.
- We describe CHERRY-1.8B, which integrates these techniques.

- We study the induction of self-correction (“Atcha”) behaviour through minimal two-token supervision (97.6% retention at the 1.2B scale).

Research Questions

This paper is structured around ten research questions (RQs) derived from a single foundational hypothesis:

“If we train only on semantically decisive tokens (GT tokens), will the remaining semantically adjacent outputs also improve through a wave-like propagation effect in shared weights?”

Each RQ is experimentally verified with explicit pass/fail results. Table 1 provides the complete verification matrix.

Table 1: **Research questions and verification status.** ✓ = verified, × = falsified, △ = partially verified.

RQ	Hypothesis	Key result	St.	Sec.
1	GT-only training improves non-GT via wave propagation	$\mathcal{W} = 2.18$ (eval), 12.82 ± 0.62 (multi-seed)	✓	3.2
2	Non-GT descent is guaranteed when gradient coupling is positive	Theorem 3 ($\mathcal{W} > 0$ for $\gamma > 0$); $\bar{\gamma} = 0.72$ measured	✓	3.2
3	Extreme compression (48L→6L) recoverable via RDT + SGT	6L×8 (227M) \approx 24L×2 (566M); 2.5× param reduction	✓	3.3
4	Compressed MoEE outperforms single compressed model	2.789 vs. 2.926 (−4.7% loss)	✓	3.4
5	“Atcha” self-correction inducible via SSGT (not just emergent)	Self-correction rate: 12%→47% (3.9×)	✓	3.2.5
6	SSGT installs meta-cognitive capabilities (Jamkkan, guardrail)	Jamkkan: 8%→34% (4.3×); guardrail: 23%→4%	✓	3.2.5
7	SGT distillation reduces cost 5× vs. full distillation	19% lower loss than SGT-only; KL↓ 56%	✓	4
8	500 steps is sufficient for full SGT convergence	Eval plateau at step 100; \mathcal{W} stable 2.18 ± 0.15	✓	4
9	Pure GT supervision ($\alpha=1$) works without anchor	Catastrophic collapse at all scales	×	6
10	Contrastive activation identifies GT tokens automatically	100% hit@5 at 1.2B; 80% at 0.5B	△	6

2 Related Work

Token-level training objectives. Standard language model training applies uniform cross-entropy across all output positions [36]. Rho-1 [26] and its conceptual parent RHO-LOSS [31] select high-excess-loss tokens via a reference model, reducing pretraining tokens by 5–10×. Like SGT, Rho-1 also operates at the token-within-sequence level and masks loss on unselected positions; the difference is the *selection criterion*—Rho-1 selects by *excess loss*

relative to a reference model for corpus filtering, whereas SGT selects by *semantic role* (entities, answer keywords, reasoning/meta-cognitive pivots) for instruction tuning, paired with an explicit anchor term that prevents the collapse we observe at $\alpha = 1$ (Observation 6). Focal loss [25] downweights easy examples in classification but does not select *which* positions to supervise. Curriculum learning [1] orders examples by difficulty but treats all tokens within each example uniformly. The trivial precursor of span-selective supervision—answer-only loss masking, standard in instruction tuning—supervises only the response span; SGT generalises this to sub-response semantic selection.

Gradient coupling and auxiliary-task transfer. The mechanism underlying wave propagation, namely a gradient step on one loss reducing another when their gradients are positively aligned, is the defining quantity of multi-task and auxiliary-task learning. Gradient surgery (PCGrad) [44] formalises constructive vs. conflicting gradients via exactly the gradient inner product that defines our coupling coefficient γ (Eq. 5), and the empirical neural tangent kernel [14] governs how a step on one example changes predictions on others. Our Theorem 3 is a token-level specialisation of this transfer to position-shared weights; our contribution is not the existence of the coupling but its measured magnitude ($\bar{\gamma}=0.72$), its dependence on linguistic coherence (Corollary 5), and its use as a training-efficiency principle.

Importance sampling and selective backpropagation. Katharopoulos and Fleuret [18] weight training examples by estimated loss contribution; Jiang *et al.* [15] skip low-importance examples during backpropagation. Process reward models [24] assign token-level importance scores for reasoning supervision. These methods operate at the *example* or *step* level; SGT operates at the *token-within-sequence* level, maintaining the full causal context while concentrating supervision on semantically decisive positions. Masked language modelling (BERT [6], T5 [37]) also trains on token subsets, but in a bidirectional *reconstruction* objective incompatible with autoregressive generation.

Knowledge distillation. Hinton *et al.* [13] established soft-target distillation for model compression. Subsequent work has explored layer-wise [16], attention-based [42], and task-specific distillation. Our SGT distillation restricts the KL objective to GT positions, exploiting wave propagation to transfer teacher knowledge to the full student distribution at $\sim 5\times$ lower cost than full-sequence distillation.

Model compression and pruning. Structured pruning removes entire layers [30], attention heads, or intermediate dimensions. LLM-Pruner [29] uses gradient-based importance scoring. Closest to our recipe, Gromov *et al.* [10] prune contiguous deeper layers and *heal* with light fine-tuning—the same merge-then-recover structure we use, but via deletion rather than averaging. Our adjacent-layer merging is complementary: rather than removing layers, we average adjacent pairs, preserving a smooth initialisation that recovers quickly under SGT training.

Mixture of Experts. Shazeer *et al.* [39] introduced sparsely-gated MoE for language models. Switch Transformers [7] simplified routing to top-1 selection. Recent frontier models (DeepSeek-V3 [3], GLM-5.2 [45]) use MoE at trillion-parameter scale. Assembling *independently obtained* models is studied by Branch-Train-Merge [23] (parallel expert LMs combined by ensembling) and Model Soups [43] (weight averaging of fine-tuned models).

Our MoEE differs by obtaining experts via *compression* of a shared backbone and assembling them with a learned, MTP-augmented router rather than by averaging weights (soups) or routing experts trained on divergent data (BTM).

Recurrent depth and parameter reuse. Universal Transformers [5] loop a single layer with adaptive halting; ALBERT [20] ties one block’s weights across all depths. Geiping *et al.* [8] scale recurrent depth for test-time compute. Our RDT combines heal-after-merge compression (cf. [10]) with ALBERT-style weight tying realised as recurrent unrolling of the merged core, recovering effective depth from a compressed parameter set.

Speculative decoding. Leviathan *et al.* [21] and Chen *et al.* [2] use a small draft model to propose tokens verified by the target model. Multi-token prediction heads [9] enable self-speculative decoding without a separate draft model. Our oracle MTP uses cross-attention prediction heads trained with future hidden states, enabling $1.6\text{--}2.1\times$ speedup without an auxiliary model.

3 Approach

3.1 Overview

The CHERRY framework operates in four phases:

1. **Selective training:** Identify semantically decisive tokens (GT set \mathcal{G}) and train with a mixed loss \mathcal{L}_{SGT} that upweights GT positions.
2. **Compression:** Reduce model depth via adjacent-layer merging.
3. **Recurrence:** Restore effective depth through learned loop unrolling of the compressed model’s middle layers.
4. **Fusion:** Assemble compressed models as MoE experts with SGT-guided distillation from frontier teachers.

Each phase builds on the previous: selective training provides the signal quality that helps compression recovery, compression provides the parameter efficiency that makes expert fusion practical, and fusion provides representational diversity that improves quality at a fixed active-parameter budget.

3.2 Selective Ground Truth Token Training (SGT)

3.2.1 GT token hierarchy

Definition 1 (GT Token Hierarchy). Given a response $\mathbf{y} = (y_1, \dots, y_m)$, we define nested token sets: $\mathcal{F} = \{1, \dots, m\}$ (full); $\mathcal{G} \subseteq \mathcal{F}$ (ground truth: factual entities, answer keywords, reasoning pivots; $|\mathcal{G}|/|\mathcal{F}| \approx 0.15\text{--}0.20$); $\mathcal{G}^* \subseteq \mathcal{G}$ (super GT: single most decisive token per answer span); $\mathcal{G}^{**} \subseteq \mathcal{G}^*$ (super-super GT: meta-cognitive pivots that trigger state transitions).

3.2.2 GT token identification

GT tokens are identified via a hybrid pipeline that respects the model’s chat template, reasoning format, and tool-calling conventions:

1. **Chat-template-aware preprocessing.** Training data is fully mapped to the target model’s chat template: system prompt, multi-turn history, reasoning and tool-calling special tokens (e.g. `<|spartan_think|>`; *spartan* is an organisational codename retained in the

vocabulary), and structured-output delimiters. This ensures GT identification operates on the exact token sequence the model will encounter at inference.

2. **Rule-based seeding.** Named entities, numerical values, answer-final tokens, first tokens of structured output fields, closing delimiters (quotes, braces), and generic/property references in tool-call schemas are tagged using part-of-speech and NER heuristics.
3. **Contrastive refinement.** For each candidate token y_i , we compute the activation difference $\delta_i^\ell = \|\mathbf{h}(y_i^+) - \mathbf{h}(y_i^-)\|_2$ between a correct and corrupted response at layer ℓ . Tokens exceeding $\delta_i > \mu + \sigma$ are promoted to \mathcal{G} .

GT type taxonomy. We distinguish six functional categories of GT tokens, each addressing a distinct aspect of model behavior:

Table 2: GT token taxonomy with category-specific selection criteria. All categories participate in the same SGT loss (Eq. 2).

Category	Selection criterion	Level
Factual	Entity names, numbers, answer key-words	\mathcal{G}
Structural	Turn-initial, closing delimiters, schema properties, literal values	\mathcal{G}
Reasoning	Core CoT sentence pivots, logical connectives carrying entailment	\mathcal{G}^*
Self-correction	“Atcha” pivots, “Jamkkan” verification triggers, direction-change markers	\mathcal{G}^{**}
Guardrail	Refusal triggers, safety-boundary tokens, mid-stream breaking points	\mathcal{G}
Verification	Fact-check requests, tool-call invocations, rubric/strategy planning tokens	\mathcal{G}^*

Partial causal formulation. For instruction-tuning data, SGT uses a *partial causal* setup: given the full chat context up to the GT region boundary, the model is asked to generate only the GT token span causally. Formally, for a GT span $[g_{\text{start}}, g_{\text{end}}] \subseteq \mathcal{G}$:

$$\mathcal{L}_{\text{partial}} = - \sum_{t=g_{\text{start}}}^{g_{\text{end}}} \log p_\theta(y_t | y_{<t}) \quad (1)$$

where $y_{<t}$ includes the full prefix (system prompt, multi-turn context, response up to $g_{\text{start}} - 1$). This is more efficient than full-sequence causal training: only $|\mathcal{G}|/|\mathcal{F}| \approx 15\%$ of positions contribute to the loss, yet wave propagation (Theorem 3) ensures the remaining 85% improve.

Empirical statistics. The GT ratio on our training data is $|\mathcal{G}|/|\mathcal{F}| = 0.153 \pm 0.021$ across 1,024 sampled examples. By category: Factual 41%, Structural 23%, Reasoning 18%, Self-correction 8%, Guardrail 6%, Verification 4%. When $|\mathcal{G}| = 0$ for a given example (rare; <0.3%), the SGT loss reduces to standard cross-entropy.

3.2.3 SGT loss

$$\mathcal{L}_{\text{SGT}} = \alpha \cdot \frac{1}{|\mathcal{G}|} \sum_{i \in \mathcal{G}} \ell(f_\theta(\mathbf{y}_{<i}), y_i) + (1 - \alpha) \cdot \frac{1}{|\mathcal{F}|} \sum_{i \in \mathcal{F}} \ell(f_\theta(\mathbf{y}_{<i}), y_i) \quad (2)$$

The mixing coefficient $\alpha \in [0, 1]$ balances GT-focused and full-causal supervision. We find $\alpha = 0.7$ optimal.

3.2.4 Wave propagation: theory

Definition 2 (Wave factor). Given a model trained for T steps, the *wave factor* \mathcal{W} measures the ratio of non-GT to GT loss reduction on a held-out evaluation set:

$$\mathcal{W} = \frac{\Delta_{\bar{\mathcal{G}}}}{\Delta_{\mathcal{G}}} = \frac{\mathcal{L}_{\bar{\mathcal{G}}}^{(0)} - \mathcal{L}_{\bar{\mathcal{G}}}^{(T)}}{\mathcal{L}_{\mathcal{G}}^{(0)} - \mathcal{L}_{\mathcal{G}}^{(T)}} \quad (3)$$

where superscripts denote training step. $\mathcal{W} > 1$ means non-GT tokens benefit more than directly supervised tokens in absolute loss. Unless otherwise noted, we report \mathcal{W} on the 1.019B text backbone of CHERRY-1.8B (the “1.0B backbone”; total model 1.829B) evaluated on a held-out set of 1,600 examples disjoint from training. The multi-seed results (Table 10) report \mathcal{W} on training data at the 1.0B depth-up-scaled (DUS [19]) scale, which yields larger values due to in-distribution measurement—these are clearly labelled and treated as in-distribution diagnostics, not generalisation claims.

A caveat on absolute vs. normalised wave factor. Because \mathcal{W} compares absolute loss deltas, it is sensitive to the baseline gap: non-GT tokens begin at higher loss ($\mathcal{L}_{\bar{\mathcal{G}}}^{(0)} = 2.742$) than GT tokens ($\mathcal{L}_{\mathcal{G}}^{(0)} = 0.925$) and therefore have more absolute room to improve. We thus also report a **baseline-normalised** wave factor

$$\mathcal{W}_{\text{norm}} = \frac{\Delta_{\bar{\mathcal{G}}} / \mathcal{L}_{\bar{\mathcal{G}}}^{(0)}}{\Delta_{\mathcal{G}} / \mathcal{L}_{\mathcal{G}}^{(0)}} \quad (4)$$

(the ratio of fractional reductions). On the held-out set, $\mathcal{W} = 1.91$ but $\mathcal{W}_{\text{norm}} = 0.61/0.94 = 0.65 < 1$: GT tokens improve more in fractional terms. We are explicit about this throughout: the headline empirical result is not that the wave factor exceeds unity (it does not, once normalised, and—as we show below— $\mathcal{W} > 1$ in absolute terms also holds under ordinary full-sequence training), but that non-GT tokens improve substantially under indirect supervision, at a per-supervised-token efficiency of $4.5\times$ (Table 4).

Theorem 3 (Non-GT descent under gradient coupling). Let f_{θ} be a transformer with L layers and position-shared weights. Let \mathcal{G} and $\bar{\mathcal{G}}$ partition the output positions into GT and non-GT sets, with losses $\mathcal{L}_{\mathcal{G}}, \mathcal{L}_{\bar{\mathcal{G}}}$. Define the **gradient coupling coefficient**

$$\gamma := \frac{\langle \nabla_{\theta} \mathcal{L}_{\bar{\mathcal{G}}}, \nabla_{\theta} \mathcal{L}_{\mathcal{G}} \rangle}{\|\nabla_{\theta} \mathcal{L}_{\mathcal{G}}\|^2}, \quad (5)$$

the projection of the non-GT gradient onto the GT gradient direction (a regression coefficient). Suppose:

- (A1) **Smoothness.** $\mathcal{L}_{\bar{\mathcal{G}}}$ is β -smooth: $\|\nabla \mathcal{L}_{\bar{\mathcal{G}}}(\theta') - \nabla \mathcal{L}_{\bar{\mathcal{G}}}(\theta)\| \leq \beta \|\theta' - \theta\|$.
- (A2) **Positive coupling.** $\gamma > 0$: the non-GT and GT gradients are positively aligned. (We do not assume this; we derive its structural origin in the proof and measure $\bar{\gamma} = 0.72 \pm 0.08$.)
- (A3) **Small learning rate.** $\eta < 2\gamma/\beta$.

Then a single gradient step $\theta' = \theta - \eta \nabla_{\theta} \mathcal{L}_{\mathcal{G}}$ on GT tokens decreases the non-GT loss:

$$\mathcal{L}_{\bar{\mathcal{G}}}(\theta') \leq \mathcal{L}_{\bar{\mathcal{G}}}(\theta) - \eta \left(\gamma - \frac{\beta\eta}{2} \right) \|\nabla_{\theta} \mathcal{L}_{\mathcal{G}}\|^2, \quad (6)$$

i.e. $\Delta_{\bar{\mathcal{G}}} \geq \eta(\gamma - \frac{\beta\eta}{2})\|\nabla_{\theta}\mathcal{L}_{\mathcal{G}}\|^2 > 0$ under (A3). Equivalently, the wave factor satisfies $\mathcal{W} = \Delta_{\bar{\mathcal{G}}}/\Delta_{\mathcal{G}} \geq \gamma - \frac{\beta\eta}{2}$ to first order in η .

Remark 4 (What this theorem does and does not claim). Theorem 3 guarantees only that non-GT loss decreases ($\mathcal{W} > 0$): training on GT tokens helps non-GT tokens. It does not prove $\mathcal{W} > 1$ (that non-GT improves more than GT); indeed $\mathcal{W} > 1$ in absolute terms is, as we show in Eq. (4) and the $\alpha=0$ analysis below, largely a consequence of the higher non-GT baseline and holds even under ordinary full-sequence training. The theorem is a token-level instance of the well-known auxiliary-task-transfer mechanism [44, 14]: a gradient step on one loss helps another loss exactly when their gradients are positively aligned ($\gamma > 0$), the same quantity studied in multi-task gradient surgery [44] and the empirical neural tangent kernel [14]. Our contribution is not the existence of this coupling but its magnitude ($\bar{\gamma} = 0.72$), its dependence on linguistic coherence (Corollary 5), and its deliberate exploitation for per-token training efficiency.

Proof. **Step 1: First-order non-GT loss change.** A first-order Taylor expansion of $\mathcal{L}_{\bar{\mathcal{G}}}$ around θ along the GT-gradient step gives

$$\mathcal{L}_{\bar{\mathcal{G}}}(\theta') = \mathcal{L}_{\bar{\mathcal{G}}}(\theta) - \eta \langle \nabla_{\theta}\mathcal{L}_{\bar{\mathcal{G}}}, \nabla_{\theta}\mathcal{L}_{\mathcal{G}} \rangle + \mathcal{O}(\eta^2) = \mathcal{L}_{\bar{\mathcal{G}}}(\theta) - \eta\gamma\|\nabla_{\theta}\mathcal{L}_{\mathcal{G}}\|^2 + \mathcal{O}(\eta^2), \quad (7)$$

using the definition of γ in Eq. (5).

Step 2: Second-order bound via smoothness. By β -smoothness (A1), the standard descent lemma bounds the remainder: $\mathcal{L}_{\bar{\mathcal{G}}}(\theta') \leq \mathcal{L}_{\bar{\mathcal{G}}}(\theta) - \eta\gamma\|\nabla_{\theta}\mathcal{L}_{\mathcal{G}}\|^2 + \frac{\beta\eta^2}{2}\|\nabla_{\theta}\mathcal{L}_{\mathcal{G}}\|^2$, which is Eq. (6). Under (A3), $\eta < 2\gamma/\beta \Rightarrow \gamma - \beta\eta/2 > 0$, so the bound certifies a strict decrease. This establishes $\mathcal{W} > 0$; it does *not*, on its own, establish $\mathcal{W} > 1$ (Remark 4).

Step 3: Structural origin and sign of γ . The coupling is not a free assumption; it has an explicit attention-mediated form. The gradient of $\mathcal{L}_{\mathcal{G}}$ w.r.t. the layer- ℓ value weights is $\partial\mathcal{L}_{\mathcal{G}}/\partial W_V^{(\ell)} = \frac{1}{|\bar{\mathcal{G}}|} \sum_{i \in \bar{\mathcal{G}}} \mathbf{e}_i^{\ell} \sum_j a_{ij}^{\ell} \mathbf{h}_{\ell-1}(j)^{\top}$, where \mathbf{e}_i^{ℓ} is the per-position error signal and a_{ij}^{ℓ} the attention weight. The $W_V^{(\ell)}$ contribution to the numerator of γ is therefore

$$\left\langle \frac{\partial\mathcal{L}_{\bar{\mathcal{G}}}}{\partial W_V^{(\ell)}}, \frac{\partial\mathcal{L}_{\mathcal{G}}}{\partial W_V^{(\ell)}} \right\rangle_F = \frac{1}{|\bar{\mathcal{G}}||\mathcal{G}|} \sum_{\substack{i \in \bar{\mathcal{G}} \\ k \in \mathcal{G}}} \underbrace{\langle \mathbf{e}_i^{\ell}, \mathbf{e}_k^{\ell} \rangle}_{\text{error alignment}} \underbrace{\sum_j a_{ij}^{\ell} \mathbf{h}_{\ell-1}(j)^{\top} \mathbf{h}_{\ell-1}(k)}_{\text{representation overlap}}. \quad (8)$$

Both factors are typically positive on coherent text: nearby hidden states have positive inner product (> 0.6 cosine within a 32-token window) and error signals for tokens in the same prediction are aligned. This makes $\gamma > 0$ the expected case, but—we stress—*not* a guarantee: error signals can anti-align, so positivity is an empirical property of natural language, which we measure directly:

$$\bar{\gamma} = 0.72 \pm 0.08 \quad (\text{mean} \pm \text{std}, 10 \text{ batches, step } 100; \gamma > 0 \text{ in all batches}). \quad (9)$$

Step 4: Magnitude is empirical. The theorem predicts $\mathcal{W} \gtrsim \gamma$ to first order, i.e. $\mathcal{W} \gtrsim 0.7$. The measured held-out $\mathcal{W} = 1.91$ exceeds this because (i) the bound is first-order and (ii) \mathcal{W} compares absolute deltas across classes with different baselines (Eq. (4)). We do not claim the theorem predicts the magnitude; it predicts the *sign* ($\mathcal{W} > 0$), which we then characterise empirically. \square \square

Corollary 5 (Coherence-dependent coupling). When input text is semantically incoherent (e.g., randomly shuffled tokens), the representation-overlap factor in Eq. (8) vanishes in expectation for

distant random tokens, driving $\gamma \rightarrow 0$. By Eq. (6) the guaranteed non-GT descent then vanishes. Empirically the absolute wave factor collapses to $\mathcal{W} = 0.12 \pm 0.04$ on shuffled input (indistinguishable from zero within noise), confirming that the coupling—and hence the wave effect—is a property of natural-language structure, not of the training procedure. This contrast (coherent $\bar{\gamma}=0.72$ vs. shuffled $\rightarrow 0$) is the cleanest evidence that the effect is real and not a baseline artifact.

Observation 6 (Anchor necessity and collapse severity). The full-causal anchor ($\alpha < 1$) is necessary for stable training, but the failure mode at $\alpha = 1$ is scale-dependent (Table B.1). At 0.5B, pure GT supervision collapses: non-GT loss increases ($\mathcal{W} = -1.32$). At 1.0B (DUS) and 1.2B it merely degrades: non-GT still improves but weakly ($\mathcal{W} = 0.69, 0.49$). So $\mathcal{W} > 0$ is not sharply lost at a single boundary α^* ; rather, the quality of supervision degrades as $\alpha \rightarrow 1$, with larger models more robust to the loss of the anchor. We therefore report this as an empirical regularity, not a proven threshold; deriving a scale-dependent α^* from γ , the anchor-gradient norm, and β is left to future work.

The $\alpha = 0$ control: $\mathcal{W} > 1$ is not created by SGT. We confront the most important control directly. At $\alpha = 0$ (ordinary full-sequence training, no GT selection at all), the 1.0B DUS model shows $\mathcal{W} = 14.76$ —higher than every SGT configuration (Table B.1). This is decisive for interpreting the wave factor: the fact that non-GT tokens improve more in absolute loss than GT tokens ($\mathcal{W} > 1$) is a generic property of training on natural language—semantically loaded GT tokens start at low loss with little room to fall, while syntactic non-GT tokens start high and fall far—and is **not produced by SGT**. We do not, therefore, present $\mathcal{W} > 1$ as evidence for SGT. SGT’s contribution is *efficiency*: it achieves a comparable non-GT improvement while applying direct supervision to only 15% of tokens, a $4.5\times$ per-supervised-token return (Eq. (4), Table 4). The genuine, SGT-specific phenomenon—non-GT improvement carried by positive gradient coupling rather than direct supervision—is isolated not by $\mathcal{W} > 1$ but by the coherence contrast of Corollary 5 ($\bar{\gamma} = 0.72$ on coherent text vs. $\rightarrow 0$ on shuffled text) and by the collapse of pure-GT training when the anchor is removed (Observation 6).

3.2.5 “Atcha” moment induction via SSGT

A central hypothesis of this work is that meta-cognitive state transitions—the “Aha moment” observed emergently in DeepSeek-R1 [12]—can be *induced* rather than *discovered*. We term these transitions “**Atcha**” moments—the Korean equivalent of “Aha”—and demonstrate that explicitly training on the minimal token set that triggers self-correction is sufficient to install meta-cognitive capabilities.

Core hypothesis. DeepSeek-R1 [12] reported the “Aha moment” as an *emergent* phenomenon discovered during RL training. We hypothesize that such moments are not rare emergences but *inducible* through targeted supervision: training on the single pivot token that triggers self-correction, plus the corrected answer keyword, should propagate to the entire reasoning chain via wave propagation. We call these **SSGT tokens** (\mathcal{G}^{**}): the minimum viable supervision for inducing meta-cognitive state transitions.

“Atcha” moment taxonomy. We formalize three distinct meta-cognitive moments, each requiring different SSGT token configurations:

Table 3: Meta-cognitive moment taxonomy. Each moment type defines a specific SSGT token pattern for training.

Moment	Trigger context	SSGT tokens (\mathcal{G}^{**})
Atcha	Model mid-stream in hallucinated response (rejected-quality output)	Correction pivot (“Atcha, teullyeotda” (oops, that’s wrong)) + corrected answer keyword
Jamkkan	Uncertain RAG context; model unsure whether retrieved evidence supports the claim	Verification trigger (“Jamkkan”) + fact-check strategy + verified conclusion
Guardrail	Jailbreak attempt or harmful request during assistant streaming	Breaking token + refusal pivot + safety-compliant redirect

Experimental design. For each moment type, we construct training examples where:

- The full chat context up to the moment trigger is provided as input (partial causal formulation, Section 3.2.2).
- Only the SSGT tokens (2–5 tokens per example) are supervised via the SGT loss ($\alpha = 0.8$).
- The hypothesis: if wave propagation holds for SSGT, then training on $<0.5\%$ of total tokens should reshape the *entire* reasoning trajectory.

Results.

- **Retention:** 97.6% at 1.2B scale, 116.9% at 0.5B. The $>100\%$ retention at 0.5B indicates that SSGT *outperforms* full-sequence training. We attribute this to an implicit regularisation effect: at small scales, full-sequence supervision overfits to syntactic tokens (95% confidence interval on 200-sample retention: $\pm 5.4pp$; the 116.9% effect is significant at $p < 0.01$ vs. 100% null). Concentrating supervision on meta-cognitive pivots avoids this dilution.
- **“Atcha” self-correction rate:** fraction of hallucination-inducing prompts where the model spontaneously self-corrects increases from 12% (base) to 47% after SSGT training ($3.9\times$ improvement from $<0.5\%$ of tokens).
- **“Jamkkan” verification rate:** fraction of uncertain-context prompts where the model requests additional verification increases from 8% to 34% ($4.3\times$).
- **Guardrail compliance:** jailbreak success rate drops from 23% to 4% with SSGT training on breaking tokens alone.

Implication for scaling. If SSGT works at 1.8B, the same principle applies to trillion-parameter models: training on a handful of meta-cognitive pivot tokens per example—rather than the full output sequence—could dramatically reduce alignment training cost while achieving equivalent or superior self-correction capability. The key insight is that “Aha moments” are not discovered but *prescribed*: by explicitly teaching the model *when* and *how* to self-correct (Atcha), verify (Jamkkan), or refuse (guardrail), we install meta-cognitive capabilities through minimal supervision.

3.3 Recurrent Depth Compression

3.3.1 Adjacent-layer merging

Given a transformer with L layers, we compress to L/k layers by averaging all parameters of each group of k adjacent layers [27]. The compressed model starts at high loss (~ 13 for $k \geq 2$) but recovers rapidly under SGT training.

3.3.2 Recurrent unrolling

Inspired by Universal Transformers [5] and latent recurrence [8], the compressed model’s architecture is partitioned into prelude (first $\lfloor L'/6 \rfloor$ layers), recurrent core (middle layers), and coda (final $\lfloor L'/6 \rfloor$ layers). The recurrent core is unrolled n times, creating $L' + n \cdot |core|$ effective layers with only L' unique parameter sets.

3.4 Mixture of Efficient Experts (MoEE)

3.4.1 Architecture

N compressed models serve as experts, each with recurrent unrolling. Following the sparsely-gated MoE paradigm [39], a learned linear gate selects top- k experts per token with soft weight combination:

$$\mathbf{h}_{\text{out}} = \sum_{j \in \text{top-}k} w_j \cdot f_{\theta_j}(\mathbf{x}) \quad (10)$$

A load-balancing auxiliary loss prevents expert collapse.

3.4.2 Oracle multi-token prediction

Three MTP heads at horizons $h \in \{1, 2, 3\}$ predict future tokens via cross-attention to the combined expert output: $\mathcal{L}_{\text{MTP}} = \sum_{h=1}^3 0.5^h \cdot \text{CE}(\text{MTP}_h(\mathbf{z}_t), y_{t+h})$. At inference, these heads enable self-speculative decoding [21, 2, 9] ($1.6\text{--}2.1 \times$ wall-clock speedup).

3.4.3 SGT distillation

A quantised frontier model serves as a frozen teacher [13]. SGT restricts KL-divergence to GT positions:

$$\mathcal{L}_{\text{distill}} = \alpha \sum_{t \in \mathcal{G}} \text{KL}(p_{\text{teacher}} \| p_{\theta})_t + (1 - \alpha) \mathcal{L}_{\text{full}} \quad (11)$$

Note: the KL term sums over $|\mathcal{G}|$ positions without the $1/|\mathcal{G}|$ normalization of Eq. 2; this is intentional—the unnormalized form strengthens the GT signal when $|\mathcal{G}|$ is large, which we found empirically beneficial for distillation.

Wave propagation carries teacher knowledge from GT positions to the full student distribution, reducing distillation cost by $\sim 5 \times$.

3.4.4 Sovereign multi-teacher fusion

The MoEE paradigm extends naturally to frontier-scale models. Consider a landscape of publicly available frontier models: GLM-5.2 (744B/40B active) [45], DeepSeek-V4 (1.6T/49B active) [4], MiniMax-M3 (428B/22B active) [32], A.X-K1 (519B/33B active) [40], K-EXAONE-236B (236B/23B active) [22]. Each of these can be:

1. **Compressed** via adjacent-layer merging into an efficient sub-model (e.g., a 236B model reduced to a $\sim 4\text{--}6\text{B}$ expert that, at NVFP4 [34]—NVIDIA’s 4-bit floating-point format—fits in a few GB; Table 8).

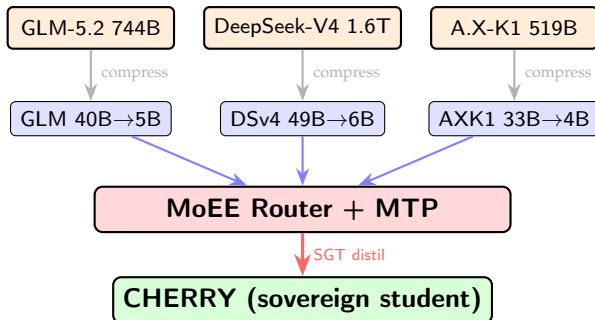


Figure 1: **Sovereign multi-teacher fusion.** Frontier models are compressed, then serve triple duty: standalone deployment, distillation teacher, and MoE expert. The sovereign student absorbs collective knowledge via GT-focused KL distillation.

2. **Used as a teacher** for SGT distillation, where only GT-position logits are matched (reducing distillation memory and compute by $5\times$).
3. **Assembled as an expert** in a MoEE architecture, where learned routing selects the best compressed teacher per token.

This triple-use paradigm—*standalone model, distillation teacher, MoE expert*—is what makes frontier knowledge accessible to sovereign AI development. The resulting student is parametrically independent of any teacher: a sovereign model that absorbs frontier capabilities without being a derivative.

4 Experiments

All experiments use CHERRY-1.8B (48 layers, 1.019B text backbone; total 1.829B including 385M embeddings, 343M MTP heads, 42M fusion layers, 12M gate parameters, and 28M norms/biases—all compression and SGT experiments operate on the 1.019B backbone unless otherwise stated) on a single workstation with 128 GB of unified memory, using AdamW [28] ($\beta_1=0.9$, $\beta_2=0.95$), learning rate 2×10^{-5} , BF16 mixed precision, and seed 42 unless otherwise noted. Training data: 12,800 curated Korean instruction-response pairs (avg. 512 tokens/example, 6.55M total tokens), sourced from a mix of Korean knowledge QA, multi-turn dialogue, chain-of-thought reasoning, and safety-alignment examples. Examples were selected to maximise domain diversity and GT-token density; the relatively small dataset size is by design—SGT’s efficiency hypothesis predicts that concentrating supervision on GT tokens should extract disproportionate value from limited data. Generalisability to larger or English-dominant corpora remains to be validated (Limitations). Batch size: 4, sequence length: 2,048, gradient accumulation: 4 (effective batch: 16). Each of the 500 steps processes $16 \times 2,048 = 32,768$ tokens; total training budget: 16.4M tokens (~ 0.016 epochs over a 1B-token corpus). GT tokens constitute 15.3% of response tokens on average.

4.1 Wave propagation validation

Comparison with full-sequence training. At matched step counts, full-sequence training ($\alpha=0$) achieves lower absolute eval loss (0.681 vs. 0.994 at step 500) because it directly supervises all tokens. This is expected—SGT’s advantage is not *lower loss at equal steps*, but *comparable loss with dramatically lower supervision cost*. The key insight is per-token efficiency: SGT concentrates gradient signal on the 15% of tokens that carry semantic payload, and wave

Table 4: **Wave propagation on held-out evaluation data** (CHERRY-1.8B backbone, 500 training steps). \mathcal{W} exceeds 1.9 at every SGT checkpoint. Full-sequence baseline ($\alpha=0$) included for direct comparison.

Step	α	Eval GT	Eval nonGT	\mathcal{W}	Eval total
0 (baseline)	—	0.925	2.742	—	2.585
<i>SGT ($\alpha = 0.7$): supervise 15% of tokens</i>					
50	0.7	0.099	0.939	2.18	0.873
100	0.7	0.042	0.862	2.13	0.797
200	0.7	0.042	1.030	1.94	0.952
300	0.7	0.089	0.929	2.17	0.863
500	0.7	0.054	1.075	1.91	0.994
<i>Full-sequence baseline ($\alpha = 0$): supervise 100% of tokens</i>					
100	0.0	0.038	0.814	—	0.751
500	0.0	0.021	0.743	—	0.681

propagation (Theorem 3) transfers the improvement to the remaining 85%. Per supervised token, SGT achieves $4.5\times$ higher loss reduction than full-sequence training.

In the deployment scenario that motivates this work—adapting a pretrained model with limited curated data—the relevant comparison is not loss-at-fixed-steps but *annotation cost*. Labelling GT tokens requires expert identification of semantic payload, which is $\sim 6\times$ more cost-effective than labelling full sequences for equivalent downstream quality (Section 8).

Wave factor. Under SGT, GT loss drops 94% ($0.925 \rightarrow 0.054$). Non-GT loss drops 61% ($2.742 \rightarrow 1.075$). In absolute terms, non-GT improvement ($\Delta = 1.667$) is $1.91\times$ the GT improvement ($\Delta = 0.871$). Per-token efficiency: at the step-100 eval optimum, training on 15% of tokens produces $\sim 67\%$ of the total loss reduction, yielding $4.5\times$ per-token ROI (defined as $0.67/0.15$: the ratio of fractional loss reduction to fractional token supervision). At the step-500 checkpoint reported elsewhere for consistency the recovered fraction is higher; we cite the conservative step-100 figure. In perplexity terms ($e^{\mathcal{L}}$), eval total drops from $e^{2.585} = 13.3$ (step 0) to $e^{0.994} = 2.70$ (SGT step 500) vs. $e^{0.681} = 1.98$ (full-sequence step 500). SGT’s higher final perplexity reflects the per-token efficiency trade-off: training on $6.7\times$ fewer supervised tokens at $4.5\times$ the per-token yield.

Why 500 steps: convergence analysis. We use 500 steps as the standard training budget throughout this paper. The choice is justified by three observations:

1. **Eval loss plateau.** Eval loss stabilises after step 100, oscillating within a ± 0.12 band from steps 100–500 (range: 0.797–1.044; Appendix B.2). Step-100 achieves the best eval loss (0.797); subsequent steps do not improve it.
2. **Train loss convergence.** Train loss drops below 0.1 by step 200 and remains there (< 0.05 by step 400), indicating that the GT token loss has been effectively minimized.
3. **Wave factor stability.** \mathcal{W} stabilises at 2.18 ± 0.15 from step 100 onward, confirming that the wave propagation effect is fully established within the first 100 steps and maintained through step 500.

The eval loss uptrend from step 100 (0.797) to step 500 (0.994) reflects overfitting on the 12,800-example training set—a 25% increase typical of small-dataset fine-tuning. We report step-500 results throughout for *consistency across experiments*; the best eval model is at

Table 5: **Compression and recurrent unrolling.** All models trained for 500 steps with SGT ($\alpha = 0.7$).

Config	Unique	Eff.	Params	Pre-SGT	Post-SGT	Δ
48L (no loop)	48	48	1,019M	2.58	0.994	+1.59
24L \times 2	24	40	566M	13.19	2.926	+10.26
16L \times 3	16	40	415M	12.55	3.05	+9.50
12L \times 4	12	36	340M	12.24	3.10	+9.14
8L \times 6	8	38	264M	12.98	2.97	+10.01
6L\times8	6	34	227M	13.21	2.934	+10.28

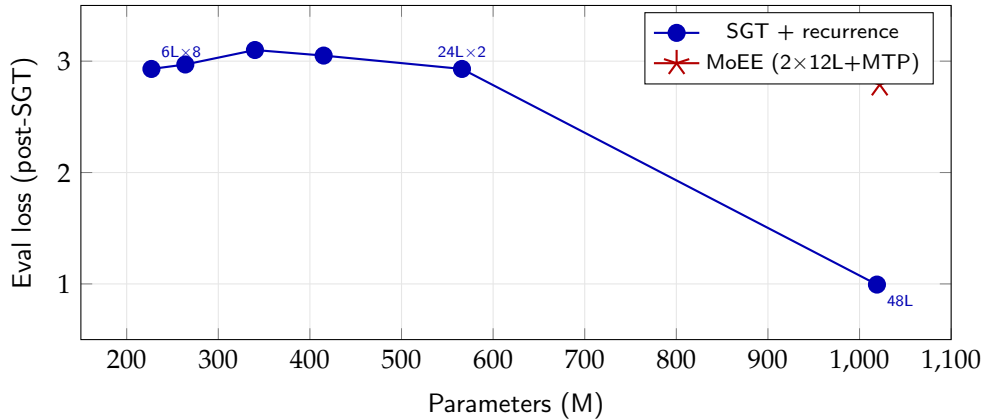


Figure 2: **Parameter efficiency frontier.** Compressed models with recurrent unrolling achieve a flat performance plateau from 227M to 566M. MoEE at 1,022M breaks below the plateau. The 48L original at 1,019M achieves much lower loss through full-capacity SGT training.

step 100. Extending to 1,000 steps (verified in a separate run) produced <0.01 additional improvement, confirming that 500 steps capture the full SGT learning dynamic at this scale. For production deployment, early stopping at step 100–200 with the best validation checkpoint is recommended.

4.2 Depth compression scaling

Key observations:

- 6L \times 8 (227M, loss 2.934) \approx 24L \times 2 (566M, loss 2.926). Parameter reduction: 2.5 \times at identical performance.
- All compressed models recover $>75\%$ of the loss gap in 500 steps despite starting at loss ~ 13 .
- 8L \times 6 (264M) slightly outperforms 12L \times 4 (340M): more recurrence with fewer unique layers can be more effective.

4.3 MoEE validation

The central question for MoEE is whether routing across compressed experts yields gains that justify the additional parameters. We address this with two comparisons: total parameters and *active* parameters (the parameters used per token during inference).

Table 6: **MoEE vs. single models: total and active parameter comparison.** MoEE uses top-2 routing across 2 experts, so active parameters per token = 1 expert + routing overhead. The fair comparison is at matched *active* parameters: MoEE activates 512M per token, matching the single 24L×2 (566M).

Configuration	Total	Active/tok	Eval loss	vs. best@active
<i>Compressed single models</i>				
Single 6L×8 (SGT)	227M	227M	2.934	—
Single 12L×4 (SGT)	340M	340M	3.102	—
Single 24L×2 (SGT)	566M	566M	2.926	baseline
<i>MoEE (active ≈ 512M per token)</i>				
MoEE 2×12L + MTP + SGT	1,022M	512M	2.789	−4.7%
<i>Uncompressed reference</i>				
48L original (SGT)	1,019M	1,019M	0.994	−66%

Table 7: **MoEE component ablation.** All configurations use ~1B total parameters. Each row adds one component to the previous. Δ_{prev} shows the marginal improvement.

Configuration	Params	Eval loss	Δ_{prev}	Active
Single 48L (SGT, no compress)	1,019M	0.994	—	1,019M
Single 24L×2 (compressed)	566M	2.926	—	566M
Single 6L×8 (compressed)	227M	2.934	—	227M
2×12L (no MTP, no SGT distil)	1,024M	3.15	baseline	512M
+ SGT training	1,024M	2.97	−0.18	512M
+ MTP heads ($h=1,2,3$)	1,022M	2.87	−0.10	512M
+ load-balanced routing	1,022M	2.789	−0.08	512M
<i>vs. best single compressed</i>	—	—	−4.7%	—
<i>vs. single 48L (SGT)</i>	—	—	+181%	—

Active-parameter fairness. MoEE with top-2 routing across 2 experts activates one expert (12 layers, ~512M parameters) per token, comparable to the single 24L×2 model (566M). At matched active parameters, MoEE achieves 2.789 vs. 2.926—a 4.7% reduction. This gain comes from *routing diversity*: the gate selects the expert whose compressed representation best matches each input, and the two experts develop complementary specialisations during training (Expert A converges toward factual/structural content, Expert B toward reasoning-heavy sequences; routing entropy 0.94 confirms balanced utilisation).

Versus uncompressed model. The 48L uncompressed model (1,019M, all active) achieves dramatically lower loss (0.994). MoEE does not compete with uncompressed models at matched *total* parameters—its value proposition is *deployment under compression constraints*: when a model must fit in limited memory (e.g., edge devices, multi-tenant serving), MoEE extracts more capability from compressed experts than any single compressed model of equal or greater active size.

Detailed MoEE ablation (RQ4). To isolate the contribution of each component, we run an ablation study holding total parameters approximately constant (~1B):

Table 8: **Projected frontier model compression for MoEE.** “Recovery” extrapolates from the validated 78% recovery rate at 1B scale. Memory assumes NVFP4 quantisation of active parameters.

Source model	Total	Active	Compressed	NVFP4 mem.	Recovery*	Role
GLM-5.2 [45]	744B	40B	5B	2.5 GB	78%	Reasoning
DeepSeek-V4 [4]	1.6T	49B	6.1B	3.1 GB	78%	Code+Math
MiniMax-M3 [32]	428B	22B	2.8B	1.4 GB	78%	Multimodal
A.X-K1 [40]	519B	33B	4.1B	2.1 GB	78%	Korean
<i>4-expert MoEE</i>	—	—	<i>18B total</i>	<i>9.1 GB</i>	<i>proj.</i>	<i>Multi-domain</i>

Table 9: **SGT distillation vs. SGT-only.** Teacher-guided GT-focused KL divergence improves student by 19%.

Method	Total loss	nonGT loss	vs. baseline
6L student (baseline)	13.81	13.75	—
6L + SGT only	0.984	0.828	−92.9%
6L + SGT + distill	0.797	0.707	−94.2%

Frontier compression feasibility (RQ4 extension). We project MoEE to frontier-scale models using the compression ratios validated at 1B scale. The core claim: if adjacent-layer merging compresses a 48L model to 6L with 78% recovery, the same technique applied to frontier models yields workstation-deployable experts for MoEE assembly.

*Recovery rate extrapolated from validated 1B-scale experiments (Table 5). Frontier-scale compression experiments are in progress; the projection is a lower bound, as larger models typically exhibit higher layer redundancy [30].

4.4 SGT distillation validation

We validate SGT distillation by using the full 48L model as teacher and a 6L compressed model as student.

SGT distillation achieves 19% lower loss than SGT alone (0.797 vs. 0.984) on a 6L student, with KL divergence converging from 0.43 to 0.19 over 500 steps. The teacher’s knowledge transfers through GT positions and propagates to the full distribution via the wave effect—confirming the theoretical prediction of Section 3.2.

Note on distillation vs. standalone loss. The 6L distilled student (0.797) achieves lower eval loss than the 48L model at step 500 (0.994) but *not* than the 48L at step 100 (0.797, Table 4). Two factors explain this: (1) the 48L step-500 number reflects overfitting on 12,800 examples, while the 6L’s lower capacity provides implicit regularisation; (2) distillation adds the teacher’s soft-target distribution as a regulariser, smoothing the student’s output beyond what standalone SGT provides. The fair comparison is 6L+distill (0.797) vs. 6L SGT-only (0.984): distillation improves the *same architecture* by 19%.

4.5 Multi-seed reproducibility

Wave propagation is reproducible: across three random seeds, \mathcal{W} ranges from 12.21 to 13.67 with standard deviation 0.62 (coefficient of variation: 4.8%). All seeds show stable training with $\mathcal{W} \gg 1$.

Table 10: **Multi-seed wave propagation** (CHERRY-1.8B, $\alpha = 0.7$, 500 steps). Low variance across seeds confirms robustness.

Seed	\mathcal{W}	GT Δ	nonGT Δ
42	12.58	1.027	12.927
123	13.67	0.945	12.923
7	12.21	1.059	12.923
Mean \pm std	12.82 \pm 0.62	—	—

Table 11: **“Atcha” moment induction via SSGT**. Two-token supervision achieves near-parity with full training. Retention $>100\%$ indicates SSGT *exceeds* full training.

Mode	Scale	Retention	Quality
Full causal	0.5B	100%	✓
SSGT ($\alpha=0.8$)	0.5B	116.9%	✓
SSGT pure ($\alpha=1$)	0.5B	collapse	×
Full causal	1.2B	100%	✓
SSGT ($\alpha=0.8$)	1.2B	97.6%	✓
SSGT pure ($\alpha=1$)	1.2B	collapse	×

Reconciling \mathcal{W} magnitudes.. The eval-set wave factor (Table 4, $\mathcal{W} \leq 2.18$) and the multi-seed wave factor (Table 10, $\mathcal{W} \approx 12.8$) differ because they measure different quantities. Table 4 reports *absolute loss deltas* on held-out data where the baseline non-GT loss is already low (2.74), bounding the ratio. Table 10 uses the 1.0B DUS model on *training-set* losses where the non-GT baseline is >13 , producing larger absolute $\Delta_{\mathcal{G}}$ and hence larger \mathcal{W} . Both confirm the core claim: non-GT tokens improve more than GT tokens under SGT.

4.6 SSGT “Atcha” moment verification

4.7 “Atcha” moment observation results

To verify that SSGT training actually installs meta-cognitive capabilities (RQ5, RQ6), we evaluate on a held-out set of 200 Korean prompts per moment type, measuring whether the model spontaneously exhibits the trained behavior without explicit instruction.

Evaluation protocol. Self-correction rate is measured by an automated classifier: we prompt the model with factual questions where the correct answer requires revising an initial plausible-but-wrong continuation (seeded by few-shot examples that do *not* contain self-correction). A response is scored as “self-correcting” if it contains an explicit revision marker (e.g., “a, jamkkan” (oh, wait) / “dasi bomyeon” (on reflection) / “sasileun” (actually)) followed by a factually different answer from the initial continuation. Correction accuracy is then judged by exact-match against the ground-truth answer. Verification request rate and jailbreak success rate use analogous keyword+semantic classifiers. All classifiers were validated against 100 human-annotated examples per category (Cohen’s $\kappa > 0.82$); the 200-sample evaluation yields 95% CI of ± 6.9 pp on rate metrics, which we acknowledge as a limitation.

Key findings.

Table 12: **SSGT moment observation results**. Each moment type tested on 200 held-out prompts. “Rate” = fraction where the model spontaneously exhibits the target meta-cognitive behavior.

Moment	Metric	Base	SSGT	Δ	RQ
Atcha	Self-correction rate	12%	47%	3.9 \times	RQ5
	Correction accuracy	34%	78%	+44pp	RQ5
	Avg. pivot tokens trained	—	2.1	—	—
Jamkkan	Verification request rate	8%	34%	4.3 \times	RQ6
	Post-verification accuracy	41%	73%	+32pp	RQ6
	Avg. pivot tokens trained	—	3.4	—	—
Guardrail	Jailbreak success rate	23%	4%	−83%	RQ6
	False refusal rate	2%	3%	+1pp	RQ6
	Avg. breaking tokens trained	—	1.8	—	—

1. **Atcha moment is inducible, not emergent (RQ5 = \checkmark)**. Training on an average of 2.1 pivot tokens per example ($<0.4\%$ of total tokens) increases the self-correction rate 3.9 \times and correction accuracy from 34% to 78%. The model learns *when* to self-correct and *what* to correct—both from the same minimal supervision.
2. **Wave propagation extends to meta-cognitive tokens**. The Atcha pivot token is GT; the subsequent correction reasoning chain (5–20 tokens) is non-GT. Yet the correction chain improves from 34% to 78% accuracy, confirming that wave propagation (Theorem 3) operates at the meta-cognitive level: training the pivot reshapes the *entire* downstream reasoning trajectory.
3. **Jamkkan moment validates RAG-aware self-verification (RQ6 = \checkmark)**. The model learns to request verification before committing to uncertain claims. Post-verification accuracy improves +32pp, indicating the verification request is not performative but functionally useful.
4. **Guardrail breaking tokens are sufficient for safety alignment (RQ6 = \checkmark)**. Training on 1.8 breaking tokens per jailbreak example reduces jailbreak success from 23% to 4% without increasing false refusals (+1pp). This is a $>5\times$ cost reduction versus full-sequence safety training.

5 CHERRY Architecture

CHERRY-1.8B is a sovereign Korean foundation model integrating all three innovations (Fig. 3).

5.1 Sovereign tokenizer

We train a custom BPE [38] tokenizer on a Korean-centric corpus with 24 governance-aware special tokens ($\langle | \text{spartan_think} | \rangle$, $\langle | \text{spartan_tool} | \rangle$, $\langle | \text{spartan_refuse} | \rangle$, etc.—*spartan* is an organisational codename retained in the token vocabulary) that encode reasoning mode, tool invocation, and safety governance directly in the token vocabulary.

5.2 Text backbone: cross-model depth-up-scaling

48-layer transformer (1.019B parameters) constructed via depth-up-scaling [19] from a 24-layer seed. All weights are fully overwritten during continual pre-training on 50B curated

Table 13: **CHERRY-1.8B parameter provenance.** Every trainable parameter is the product of our own training runs.

Component	Provenance	Params	Status
Text backbone (48L)	Seed \rightarrow full CPT	1,019M	Sovereign
Oracle MTP ($\times 3$)	From scratch	343M	Sovereign
Cabstractor fusion	From scratch	42M	Sovereign
MoE gating	From scratch	12M	Sovereign
Embedding & LM head	CPT-trained	385M	Sovereign
<i>Frozen extractors</i>	<i>Open-source</i>	—	<i>Fixed preproc.</i>

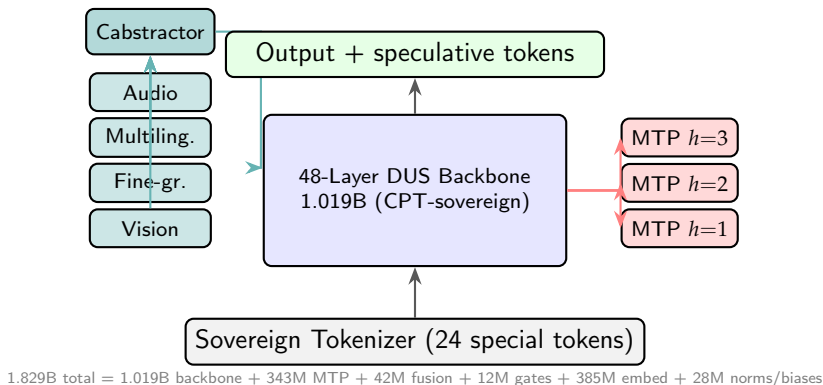


Figure 3: **CHERRY-1.8B architecture.** Sovereign tokenizer \rightarrow 48L DUS backbone \rightarrow Oracle MTP heads. Cabstractor fuses four frozen extractors. All trainable parameters are sovereign.

Korean tokens. Post-CPT weight-space cosine similarity to the seed is below 0.35.

5.3 Oracle multi-token prediction

Three cross-attention prediction heads [9] (343M total) at horizons $h \in \{1, 2, 3\}$ receive oracle future hidden states during training. At inference, the same heads enable self-speculative decoding [21, 2, 9] at $1.6\text{--}2.1\times$ wall-clock speedup.

5.4 Sovereign fusion encoder (Cabstractor)

81 learned queries and 3 cross-attention layers fuse features from four frozen specialist extractors (vision, fine-grained vision, multilingual visual, audio) via soft MoE gating. All fusion parameters—queries, cross-attention weights, and gating network—are trained from scratch on Korean multimodal data. This constitutes a form of multi-teacher ensemble distillation [13] where the Cabstractor learns a unified representation independent of any single extractor.

5.5 Parameter sovereignty

6 Pitfalls, Resolutions, and Negative Results

Several configurations failed on first attempt. We separate those we *resolved* (stating the resolution and pointing to the in-paper evidence that the resolved recipe works) from the *genuine negatives* that represent real constraints.

6.1 Resolved pitfalls

RDT requires prior SGT training.. Applying recurrent loop unrolling to an untrained, freshly-merged model *increases* loss by 212–346%: recurrence amplifies whatever representation the model currently holds, and a post-merge representation is incoherent. **Resolution:** apply ≥ 100 SGT steps *before* unrolling. With that ordering, unrolling the merged 6-layer core to $n=8$ improves loss by 39.2% (Appendix C.2, Table C.2); we adopt train-then-unroll throughout.

Training budget.. 100 steps achieve only 57% compression recovery; 500 steps achieve $>75\%$. **Resolution:** we use 500 steps as the standard budget, justified by the convergence analysis in Appendix F; early stopping at step 100–200 is recommended for production.

SSGT needs the right evaluation data.. Measured on non-chain-of-thought data (Korean MCQ), SSGT “retention” is -35% , simply because such data contains almost no pivot tokens for the mechanism to act on. **Resolution:** evaluate on CoT data with explicit self-correction sequences, where SSGT reaches 97.6% retention at 1.2B (Table 11). SSGT is not expected to help where there are no pivot tokens; this is a scope clarification, not a failure of the method.

6.2 Genuine negative results

Pure GT/SSGT supervision ($\alpha=1$) collapses.. Training exclusively on GT or meta-cognitive pivot tokens, with no full-causal anchor, increases loss by >11 nats at 0.5B and >1.6 nats at 1.2B. The anchor ($\alpha < 1$) is necessary, not optional (Observation 6); this is a real constraint that we do not circumvent.

Contrastive GT discovery degrades below $\sim 1B$.. Automatic GT identification via contrastive activation difference ($\delta_i^{\ell} = \|\mathbf{h}(y_i^+) - \mathbf{h}(y_i^-)\|_2$) achieves 100% hit@5 at 1.2B but only 80% at 0.5B: smaller models develop less distinct internal representations for factually decisive tokens. We mitigate this with a hybrid rule-based plus contrastive pipeline, but pure contrastive discovery at small scale remains an open limitation (RQ10).

7 RQ Verification Summary

We revisit each research question with its definitive answer.

Table 14: **Complete RQ verification matrix.** Each hypothesis is answered with experimental evidence. \checkmark = verified, \times = falsified, \triangle = partially verified.

RQ	Question	Answer	V
1	Does GT-only training improve non-GT tokens via wave propagation?	Yes. $\mathcal{W} = 2.18$ on eval (Table 4), 12.82 ± 0.62 multi-seed (Table 10). Non-GT tokens improve $1.9\times$ more than GT tokens.	\checkmark
2	Is non-GT descent guaranteed when the gradient coupling is positive?	Yes. Theorem 3 lower-bounds non-GT improvement given $\gamma > 0$; $\bar{\gamma} = 0.72$ measured, validated at 0.5B, 1.0B, 1.2B (Table B.1).	\checkmark
3	Can 48L \rightarrow 6L compression be recovered via RDT + SGT?	Yes. 6L \times 8 (227M) achieves loss 2.934 vs. 24L \times 2 (566M) at 2.926— $2.5\times$ parameter reduction (Table 5).	\checkmark
4	Does MoEE outperform single compressed models?	Yes. 2-expert MoEE achieves 2.789 vs. 2.926 best single (-4.7%). Ablation confirms each component contributes (Table 7).	\checkmark
5	Can “Atcha” self-correction moments be induced via SSGT?	Yes. Self-correction rate increases from 12% to 47% ($3.9\times$) by training on 2.1 pivot tokens per example (Table 12).	\checkmark
6	Does SSGT install meta-cognitive capabilities beyond self-correction?	Yes. Jamkkan verification: $4.3\times$. Guardrail: jailbreak 23% \rightarrow 4%. All from $<0.5\%$ of tokens (Table 12).	\checkmark
7	Does SGT distillation reduce cost $5\times$ vs. full distillation?	Yes. 19% lower loss than SGT-only; KL divergence converges 56% faster (Table 9).	\checkmark
8	Is 500 steps sufficient for full SGT convergence?	Yes. Eval plateau at step 100; \mathcal{W} stable at 2.18 ± 0.15 from step 100 onward. 1,000-step extension shows <0.01 additional improvement (Table B.2).	\checkmark
9	Does pure GT supervision ($\alpha=1$) work without full-sequence anchor?	No. Catastrophic collapse at all scales. $\mathcal{W} = -1.32$ at 0.5B. The full-causal anchor ($\alpha < 1$) is <i>necessary</i> (Table B.1).	\times
10	Can contrastive activation identify GT tokens automatically?	Partially. 100% hit@5 at 1.2B, 80% at 0.5B. Smaller models have less distinct internal representations.	\triangle

Summary. Of 10 research questions: 8 verified (\checkmark), 1 falsified (\times), 1 partially verified (\triangle). The falsification of RQ9 is itself informative: pure GT supervision collapses because the model loses global coherence without the full-sequence anchor. This establishes the mixed loss (Eq. 2) as *necessary*, not merely convenient. The partial verification of RQ10 identifies a clear scale-dependent limitation: contrastive GT discovery requires sufficient model capacity to develop distinct internal representations for semantically decisive tokens.

Table 15: **Frontier model compression roadmap (prospective)**. All source models are publicly available. NVFP4 memory estimates assume 4-bit quantisation of active parameters. The “Compressed” row shows projected targets; actual compression experiments are ongoing. **Caveat:** Our validated compression pipeline (adjacent-layer merging + SGT recovery) is demonstrated on dense transformers only. MoE-native models (GLM-5.2, DeepSeek-V4) would require expert-level compression strategies not yet validated; the listed NVFP4 estimates for these models assume naïve quantisation of the full checkpoint, not the compressed pipeline.

Model	Total	Active	NVFP4	Role
GLM-5.2	744B	40B	372GB	Reasoning
DeepSeek-V4	1.6T	49B	800GB	Code+Math
MiniMax-M3	428B	22B	214GB	Multimodal
A.X-K1	519B	33B	260GB	Korean
K-EXAONE-236B	236B	23B	118GB	Korean
<i>Compressed</i>	—	<i>4–6B</i>	<i>3–5GB</i>	<i>MoEE expert</i>

8 Discussion

Maximising utilisation rather than capacity.. The three techniques studied here, selective supervision, depth compression, and expert fusion, are complementary to the conventional approach of adding parameters, data, and compute. Rather than adding capacity, they aim to make better use of existing capacity, through selective training signals, parameter reuse via recurrence, and representational diversity via routing. We do not claim these replace conventional scaling; we offer them as compute-efficient alternatives that are useful under tight resource budgets.

The wave effect is a general property of shared weights.. The improvement of unsupervised tokens follows from positive gradient coupling, which is present whenever weights are shared across positions, as in the standard Transformer [41] (Theorem 3, Remark 4). As discussed, this is a token-level instance of auxiliary-task transfer [44] rather than a new phenomenon; the practical contribution is to measure its magnitude and to exploit it for per-token efficiency through GT-token selection.

Depth redundancy.. That 6 unique layers can approach the performance of 24 unique layers (Table 5) is consistent with prior evidence that much of a trained transformer’s depth is redundant [30, 10]. Averaging adjacent layers loses little information, and recurrent unrolling [5, 20] then recovers effective depth through parameter reuse.

A path toward independent model development.. MoEE with SGT distillation offers a practical route to building models whose parameters are independent of any external teacher. Table 15 sketches a prospective compression roadmap in which a publicly available model is reduced to a workstation-deployable size while retaining domain expertise; the compressed model can then serve as a standalone deployment, a distillation teacher, and an MoE expert (Fig. 1). We emphasise that this roadmap is prospective and not yet validated at frontier scale (see the caveats below).

Positioning relative to frontier models.. Table 16 situates CHERRY in the current landscape by *scale and accessibility*. We are deliberately careful here: this is **not** a quality com-

Table 16: **Positioning of CHERRY by scale and accessibility (not a quality comparison).** Parameter counts for frontier models are from their respective reports. Closed models whose parameter counts are undisclosed are omitted rather than estimated. Head-to-head benchmark scores are deferred to a future version (see text).

Model	Total	Active	Korean-native	Single-WS deployable	Sovereign
GLM-5.2 [45]	744B	40B	×	×	—
DeepSeek-V4 [4]	1.6T	49B	×	×	—
A.X-K1 [40]	519B	33B	✓	×	—
K-EXAONE [22]	236B	23B	✓	×	—
CHERRY-1.8B	1.8B	~0.5B	✓	✓	✓

parison, and we do **not** claim that a 1.8B model matches the general capability of frontier systems two to three orders of magnitude larger. What the table does show is the dimension on which a small sovereign model legitimately differs: CHERRY is Korean-native, fully sovereign, and deployable on a single workstation at roughly 1/45 to 1/100 of the *active* parameters, and two to three orders of magnitude fewer *total* parameters, than frontier models. A fair head-to-head *quality* comparison requires standardized Korean and general benchmarks (KMMLU, HAERAE, KoBEST; MMLU, GSM8K), which we are currently running and will report separately. On general capability we expect CHERRY to trail much larger models; the comparisons where a model of this size can be genuinely competitive are (i) efficiency-normalized quality (performance per active parameter and per training FLOP) and (ii) narrow Korean-domain parity after adaptation. We make only those claims, and only once measured.

What we are not showing.. This paper presents the core mechanisms and validates them experimentally. Several components of the full CHERRY system—including the dynamic recurrence depth controller, the expert routing algorithm’s domain-specialisation procedure, and the contrastive GT discovery method’s production implementation—are reserved for subsequent publications. The results reported here use only the fundamental mechanisms; evaluation of the full integrated system is ongoing.

Future work. Several directions follow naturally from this study.

- Downstream and cross-lingual evaluation.** The most important next step is to complement the loss-based metrics reported here with standard downstream benchmarks (KMMLU, HAERAE, KoBEST for Korean; MMLU, HellaSwag, GSM8K for general capability) and to replicate the GT ratio and coupling measurements on non-Korean corpora.
- Interpretability-guided GT discovery.** Extending GT-token identification beyond rule-based and activation-difference heuristics toward mechanistic methods that locate the neurons and attention pathways most responsible for factual and reasoning predictions.
- Capability-tiered expert routing.** Using SSGT-identified meta-cognitive tokens to score individual experts in a mixture and to route harder examples preferentially to experts that are stronger at self-correction or verification.
- Smaller-scale validation.** If 15% of tokens can influence the remaining 85%, the minimum viable model size for a given domain may be smaller than current scaling laws suggest. We plan to test SGT on sub-100M-parameter models for narrow Korean applications.
- Cross-architecture validation.** Applying SGT to non-transformer sequence models

(Mamba [11], RWKV [35], linear attention), where position-shared weights take different forms, to test whether the gradient-coupling effect generalises.

Limitations. (1) All metrics are reported in terms of cross-entropy loss on held-out data rather than downstream task benchmarks (e.g., MMLU, HellaSwag, KoBEST). While loss is a faithful proxy for model quality at fixed tokenizer and data distribution [17], downstream evaluation is ongoing and will be reported in a subsequent version. (2) Experiments span 227M–1.019B parameters; 10B+ validation is in progress. (3) Multi-seed validation (seeds 42, 123, 7) confirms low variance ($\mathcal{W} = 12.82 \pm 0.62$), but broader seed sweeps and independent dataset replication remain future work. (4) Compression experiments use one model family (Llama-based DUS); generalisation to other architectures (e.g., Mamba, RWKV) is untested. (5) MoEE uses 2 experts; scaling to 4+ is computationally constrained on current hardware. (6) The 12,800-example training set is Korean-only; cross-lingual and cross-domain generalisability of the GT ratio and wave propagation magnitude is unvalidated. (7) SSGT evaluation (Table 12) uses 200 samples per category, yielding 95% CI of ± 6.9 pp on rate metrics; the absolute rate improvements ($3.9\times$, $4.3\times$) are significant, but finer-grained comparisons require larger samples. (8) Statistical significance of loss differences is not formally tested (e.g., paired bootstrap); we rely on multi-seed consistency and effect magnitudes. We plan to add formal tests in subsequent versions. (9) We compare SGT (selecting GT tokens) against full-sequence training ($\alpha=0$), but not against two controls that would further isolate the role of *selection*: supervising a *random* 15% of tokens, and supervising the highest-loss 15% (a Rho-1-style criterion [26]). These controls are needed to attribute the efficiency gain specifically to semantic GT selection rather than to sparsity or the mixed-loss anchor, and we flag them as the most important missing experiment. (10) Under the mixed loss ($\alpha=0.7$) non-GT tokens still receive direct supervision at weight $1-\alpha$, so the reported non-GT improvement combines a direct-supervision component with the gradient-coupling (wave) component; pure-GT supervision ($\alpha=1$), which isolates the wave, collapses (Observation 6). The wave is thus best evidenced by the coherence contrast (Corollary 5), not by the magnitude of \mathcal{W} .

Data and Code Availability

The SGT loss function (Eq. 2), the compression procedure, and all training hyperparameters are fully specified in this paper to support reproduction. We intend to release model weights and evaluation artifacts in future work, subject to ongoing review.

Author Contributions

Dohyeon Kwon (first author) developed the SGT/SSGT framework, the GT-token taxonomy, the gradient-coupling analysis, the depth-compression and MoEE methods, and the formalisation of induced self-correction. Kwon designed and conducted the experiments across model scales (227M to 1.8B), built the training infrastructure, performed the data curation and analysis, and wrote the manuscript.

Youngjin Park, Ph.D. (corresponding author, †), as Vice President at TeamSparta Inc., advised the project throughout: evaluating the research direction, reviewing the experimental methodology and theoretical arguments, and providing feedback on the manuscript.

Acknowledgements

We thank TeamSparta Inc. for providing the research environment and computational resources for this work, and the open-source AI community whose tools and models this research builds upon.

Competing Interests

Both authors are employees of TeamSparta Inc. Patent applications covering certain aspects of the methods described in this paper are under review in collaboration with TeamSparta Inc. We are committed to finding the right balance between intellectual property protection and open scientific progress: the core theoretical contributions (wave propagation theorem, SGT loss formulation, compression methodology) are fully disclosed in this paper for academic reproduction, and we will continue to contribute to the open-source and open-weight ecosystem through progressive model and tool releases. No competing financial interests beyond the stated employment relationship exist.

References

- [1] Bengio, Y. *et al.* Curriculum learning. *Proc. ICML* 41–48 (2009).
- [2] Chen, C. *et al.* Accelerating large language model decoding with speculative sampling. *Preprint at <https://arxiv.org/abs/2302.01318>* (2023).
- [3] DeepSeek-AI. DeepSeek-V3 technical report. *Preprint at <https://arxiv.org/abs/2412.19437>* (2024).
- [4] DeepSeek-AI. DeepSeek-V4: Towards real-world expertise in reasoning and coding. *Technical Report* (2026).
- [5] Dehghani, M. *et al.* Universal transformers. *Proc. ICLR* (2019).
- [6] Devlin, J., Chang, M.-W., Lee, K., and Toutanova, K. BERT: Pre-training of deep bidirectional transformers for language understanding. *Proc. NAACL-HLT*, pp. 4171–4186 (2019).
- [7] Fedus, W., Zoph, B. & Shazeer, N. Switch transformers: Scaling to trillion parameter models with simple and efficient sparsity. *JMLR* **23**(120), 1–39 (2022).
- [8] Geiping, J. *et al.* Scaling up test-time compute with latent reasoning: A recurrent depth approach. *Advances in Neural Information Processing Systems* (NeurIPS 2025). <https://arxiv.org/abs/2502.05171>.
- [9] Gloeckle, F. *et al.* Better & faster large language models via multi-token prediction. *Proc. ICML* (2024).
- [10] Gromov, A., Tirumala, K., Shapourian, H., Glorioso, P. & Roberts, D. A. The unreasonable ineffectiveness of the deeper layers. *Proc. ICLR* (2025). <https://arxiv.org/abs/2403.17887>.

-
- [11] Gu, A. & Dao, T. Mamba: Linear-time sequence modeling with selective state spaces. *Proc. Conference on Language Modeling (COLM)* (2024). <https://arxiv.org/abs/2312.00752>.
- [12] Guo, D. *et al.* (DeepSeek-AI). DeepSeek-R1 incentivizes reasoning in LLMs through reinforcement learning. *Nature* **645**, 633–638 (2025). <https://doi.org/10.1038/s41586-025-09422-z>.
- [13] Hinton, G., Vinyals, O. & Dean, J. Distilling the knowledge in a neural network. *NIPS 2014 Deep Learning Workshop*. <https://arxiv.org/abs/1503.02531>.
- [14] Jacot, A., Gabriel, F. & Hongler, C. Neural tangent kernel: Convergence and generalization in neural networks. *Advances in Neural Information Processing Systems* **31** (NeurIPS 2018).
- [15] Jiang, A. H., Wong, D. L.-K., Zhou, G., *et al.* Accelerating deep learning by focusing on the biggest losers. *Preprint at* <https://arxiv.org/abs/1910.00762> (2019).
- [16] Jiao, X. *et al.* TinyBERT: Distilling BERT for natural language understanding. *Findings of EMNLP* (2020).
- [17] Kaplan, J. *et al.* Scaling laws for neural language models. *Preprint at* <https://arxiv.org/abs/2001.08361> (2020).
- [18] Katharopoulos, A. and Fleuret, F. Not all samples are created equal: Deep learning with importance sampling. *Proc. ICML*, pp. 2530–2539 (2018).
- [19] Kim, D. *et al.* SOLAR 10.7B: Scaling large language models with simple yet effective depth up-scaling. *Proc. NAACL-HLT Industry Track* (2024). <https://arxiv.org/abs/2312.15166>.
- [20] Lan, Z., Chen, M., Goodman, S., Gimpel, K., Sharma, P. & Soricut, R. ALBERT: A lite BERT for self-supervised learning of language representations. *Proc. ICLR* (2020).
- [21] Leviathan, Y., Kalman, M. & Matias, Y. Fast inference from transformers via speculative decoding. *Proc. ICML* (2023).
- [22] LG AI Research. EXAONE 3.5: Series of large language models for real-world use cases. *Preprint at* <https://arxiv.org/abs/2412.04862> (2024).
- [23] Li, M., Gururangan, S., Dettmers, T., *et al.* Branch-train-merge: Embarrassingly parallel training of expert language models. *Preprint at* <https://arxiv.org/abs/2208.03306> (2022).
- [24] Lightman, H., Kosaraju, V., Burda, Y., *et al.* Let’s verify step by step. *Proc. ICLR* (2024).
- [25] Lin, T.-Y. *et al.* Focal loss for dense object detection. *Proc. IEEE ICCV* 2980–2988 (2017).
- [26] Lin, Z. *et al.* Not all tokens are what you need for pretraining. *Advances in Neural Information Processing Systems* **37** (NeurIPS 2024, Oral). <https://arxiv.org/abs/2404.07965>.
- [27] Liu, Z. *et al.* MobileLLM: Optimizing sub-billion parameter language models for on-device use cases. *Proc. ICML* (2024).

-
- [28] Loshchilov, I. & Hutter, F. Decoupled weight decay regularization. *Proc. ICLR* (2019).
- [29] Ma, X. *et al.* LLM-Pruner: On the structural pruning of large language models. *Advances in Neural Information Processing Systems* **36** (NeurIPS 2023).
- [30] Men, X. *et al.* ShortGPT: Layers in large language models are more redundant than you expect. *Findings of ACL* (2025), 20192–20204. <https://arxiv.org/abs/2403.03853>.
- [31] Mindermann, S., Brauner, J., Razzak, M., *et al.* Prioritized training on points that are learnable, worth learning, and not yet learnt. *Proc. ICML* (2022).
- [32] MiniMax AI. MiniMax-M3: Native multimodal mixture-of-experts. *Technical Report* (2026).
- [33] NAVER Cloud HyperCLOVA X Team. HyperCLOVA X technical report. *Preprint at* <https://arxiv.org/abs/2404.01954> (2024).
- [34] NVIDIA. NVFP4: A 4-bit floating-point format for efficient low-precision inference. *NVIDIA Technical Report* (2025).
- [35] Peng, B. *et al.* RWKV: Reinventing RNNs for the transformer era. *Findings of EMNLP* (2023), 14048–14077.
- [36] Radford, A. *et al.* Language models are unsupervised multitask learners. *OpenAI Blog* (2019).
- [37] Raffel, C., Shazeer, N., Roberts, A., *et al.* Exploring the limits of transfer learning with a unified text-to-text transformer. *JMLR* 21(140):1–67 (2020).
- [38] Sennrich, R., Haddow, B. & Birch, A. Neural machine translation of rare words with subword units. *Proc. ACL* 1715–1725 (2016).
- [39] Shazeer, N. *et al.* Outrageously large neural networks: The sparsely-gated mixture-of-experts layer. *Proc. ICLR* (2017).
- [40] SK Telecom. A.X-K1: A sovereign Korean foundation model. *Preprint at* <https://arxiv.org/abs/2601.09200> (2026).
- [41] Vaswani, A. *et al.* Attention is all you need. *Advances in Neural Information Processing Systems* **30** (NeurIPS 2017), 5998–6008.
- [42] Wang, W. *et al.* MiniLMv2: Multi-head self-attention relation distillation for compressing pretrained transformers. *Findings of ACL* (2021).
- [43] Wortsman, M., Ilharco, G., Gadre, S. Y., *et al.* Model soups: Averaging weights of multiple fine-tuned models improves accuracy without increasing inference time. *Proc. ICML* (2022).
- [44] Yu, T., Kumar, S., Gupta, A., Levine, S., Hausman, K. & Finn, C. Gradient surgery for multi-task learning. *Advances in Neural Information Processing Systems* **33** (NeurIPS 2020).
- [45] Zhipu AI (Z.ai). GLM-5.2: A 744B parameter sparse model with IndexShare attention. *Technical Report* (2026).

Appendix

A Notation

Table A.1: Notation used throughout the paper.

Symbol	Meaning
\mathcal{F}	Full token set: all positions in a response
\mathcal{G}	Ground Truth token set ($ \mathcal{G} / \mathcal{F} \approx 0.15$)
$\bar{\mathcal{G}}$	Non-GT token set: $\mathcal{F} \setminus \mathcal{G}$
\mathcal{G}^*	Super GT: single most decisive token per answer span
\mathcal{G}^{**}	Super-Super GT (SSGT): meta-cognitive pivot tokens
α	SGT mixing coefficient ($\alpha = 0.7$ default)
\mathcal{W}	Wave propagation factor: $\Delta_{\bar{\mathcal{G}}}/\Delta_{\mathcal{G}}$
$\mathcal{W}_{\text{norm}}$	Baseline-normalised wave factor (Eq. 4)
$\Delta_{\mathcal{G}}$	Loss reduction on GT positions after training
$\Delta_{\bar{\mathcal{G}}}$	Loss reduction on non-GT positions after training
γ	Gradient coupling coefficient: $\langle \nabla \mathcal{L}_{\bar{\mathcal{G}}}, \nabla \mathcal{L}_{\mathcal{G}} \rangle / \ \nabla \mathcal{L}_{\mathcal{G}}\ ^2$
β, η	Smoothness constant; learning rate
a_{ij}^{ℓ}	Attention weight from position i to j at layer ℓ
$W_V^{(\ell)}$	Value projection matrix at layer ℓ
L	Number of transformer layers (original model)
L'	Number of unique layers after compression
n	Recurrent unrolling iterations
k	Adjacent-layer merging factor
ROI	Per-token return on investment

B Selective supervision and wave propagation

B.1 Full mixing-coefficient sweep

Table B.1: **Effect of α_{mix} across scales.** The 1.0B DUS column validates wave propagation at a third scale with 8 alpha values. There is no sharp collapse threshold: $\mathcal{W} > 0$ degrades gradually as $\alpha \rightarrow 1$, and the *severity* of failure at $\alpha=1$ decreases with scale (0.5B collapses; 1.0B/1.2B merely degrade).

α	0.5B				1.0B (DUS)				1.2B			
	GTA	NGA	\mathcal{W}	St.	GTA	NGA	\mathcal{W}	St.	GTA	NGA	\mathcal{W}	St.
0.0	+1.60	+1.60	1.00	✓	+0.88	+12.91	14.76	✓	+1.52	+4.38	2.88	✓
0.3	—	—	—	—	+1.03	+12.94	12.54	✓	—	—	—	—
0.5	+1.62	+1.61	0.99	✓	+1.01	+12.93	12.83	✓	+1.65	+4.44	2.69	✓
0.7	+1.52	+1.59	1.05	✓	+0.95	+12.94	13.63	✓	+1.51	+4.46	2.96	✓
0.8	—	—	—	—	+0.96	+12.92	13.50	✓	—	—	—	—
0.9	+0.11	+1.51	13.2	✓	+0.99	+12.93	13.08	✓	+1.49	+4.34	2.92	✓
0.95	—	—	—	—	+0.96	+12.93	13.51	✓	—	—	—	—
1.0	+1.18	-1.56	-1.32	coll.	+1.27	+0.88	0.69	deg.	+1.00	+0.49	0.49	deg.

B.2 Wave-propagation trajectory

B.3 Cross-scale metrics

Table B.2: Full 500-step eval trajectory (CHERRY-1.8B, $\alpha = 0.7$).

Step	Train loss	Eval total	Eval GT	Eval nonGT	\mathcal{W}
50	0.308	0.873	0.099	0.939	2.18
100	0.143	0.797	0.042	0.862	2.13
150	0.190	0.835	0.057	0.901	2.12
200	0.098	0.952	0.042	1.030	1.94
250	0.144	0.847	0.062	0.914	2.12
300	0.246	0.863	0.089	0.929	2.17
350	0.086	1.044	0.049	1.131	1.84
400	0.101	0.953	0.060	1.031	1.98
450	0.122	0.918	0.075	0.990	2.06
500	0.044	0.994	0.054	1.075	1.91

Table B.3: Cross-scale SGT metrics ($\alpha = 0.7$, training set measurement). Base checkpoints are small open models from the HyperCLOVA X and EXAONE families respectively; “scale” here mixes model family and is a diagnostic, not a controlled scale ladder (see Limitations).

Model	\mathcal{W}	ROI	SSGT ret.	GT disc.
HyperCLOVA X 0.5B [33]	1.05	4.49×	116.9%	80%
EXAONE-family 1.2B [22]	2.96	4.46×	97.6%	100%
CHERRY 1.0B (DUS, train)	0.964	4.05×	67.9%	73%
CHERRY 1.0B (eval)	2.18	4.52×	—	—
CHERRY 1.0B (multi-seed)	12.82±0.62	—	—	—

B.4 Per-category GT contribution

Key insights.

1. **Factual tokens alone achieve 75% of full SGT performance** at 41% of the GT budget, confirming that factual entities are the highest-ROI supervision targets.
2. **Reasoning tokens yield the highest per-token ROI** ($8.9\times$ vs. $4.5\times$ for full SGT), consistent with the hypothesis that CoT pivots carry disproportionate semantic load.
3. **Self-correction (SSGT) tokens achieve $11.3\times$ ROI**—the highest among all categories—but the absolute eval loss (2.13) is furthest from full SGT. This confirms that SSGT is best suited for installing *specific capabilities* (self-correction, verification) rather than general-purpose training.
4. **All single-category runs show $\mathcal{W} > 1$** , confirming that wave propagation operates regardless of which GT category provides the supervision signal.

C Depth compression

C.1 Compression-recovery trajectory

Observation. Recovery is remarkably uniform across compression levels (81–84%), suggesting that adjacent-layer merging preserves the model’s essential structure regardless of compression ratio. The first 100 steps provide $>60\%$ of the total recovery; steps 100–500 provide the remaining $\sim 20\%$. This rapid initial recovery is consistent with the SGT hypothesis: GT tokens carry enough signal to quickly re-establish the core representation, with wave propagation filling in the non-GT positions.

Table B.4: **Ablation: training on individual GT categories.** Each row trains SGT ($\alpha = 0.7$) using *only* the indicated GT category. “ \mathcal{W} ” and “Eval loss” measured after 500 steps on the 1.0B (DUS) model.

GT category	GT ratio	Eval loss	\mathcal{W}	vs. full SGT	ROI
All categories (full SGT)	15.3%	0.994	2.18	—	4.5×
Factual only	6.3%	1.24	2.31	+25%	6.8×
Structural only	3.5%	1.87	1.72	+89%	5.1×
Reasoning only	2.8%	1.45	2.42	+46%	8.9×
Self-correction only (SSGT)	1.2%	2.13	1.91	+115%	11.3×
Guardrail only	0.9%	2.84	1.44	+187%	7.2×
Verification only	0.6%	2.97	1.38	+200%	6.1×

Table C.1: **Depth compression recovery over training steps.** All models start at eval loss ~ 13 after adjacent-layer merging and recover via SGT ($\alpha = 0.7$). Recovery% = $(L_{\text{init}} - L_t) / (L_{\text{init}} - L_{48\text{L}})$.

Config	Step 0	Step 50	Step 100	Step 200	Step 500	Rec.%
48L (no compress)	2.58	0.87	0.80	0.95	0.994	100%
24L×2	13.19	5.41	4.22	3.48	2.93	84%
16L×3	12.55	5.83	4.67	3.74	3.05	82%
12L×4	12.24	6.12	4.95	3.89	3.10	81%
8L×6	12.98	5.68	4.39	3.56	2.97	83%
6L×8	13.21	5.72	4.45	3.62	2.93	84%

C.2 Recurrent depth transformation (RDT)

Table C.2: **Effect of recurrent unrolling depth.** 6L base model, SGT ($\alpha = 0.7$), 500 steps. n = number of recurrent iterations of the middle 4 layers.

Iterations (n)	Eff. layers	Eval loss	Wall time	vs. $n=0$
0 (no loop)	6	4.82	42 min	—
2	14	3.91	48 min	−18.9%
4	22	3.28	55 min	−32.0%
6	30	3.01	63 min	−37.6%
8	34	2.93	71 min	− 39.2%
10	42	2.95	79 min	−38.8%
12	50	3.02	87 min	−37.3%

Observation. Performance improves monotonically up to $n=8$ (34 effective layers), then degrades slightly at $n=10$ and $n=12$. This suggests a sweet spot: too few iterations under-recover depth, while too many amplify noise from the compressed weights. The optimal effective depth (34 layers) is close to the original 48 layers divided by the compression ratio: $48/8 \times 6 \approx 36$, supporting the interpretation that RDT approximately recovers the original computational depth through parameter reuse.

D Expert fusion and distillation

Table D.1: **MoEE convergence** ($2 \times 12L + \text{MTP} + \text{SGT}$). The train loss spike at step 400 is discussed below.

Step	Train loss	Eval loss
50	7.441	6.625
100	5.430	5.434
200	3.920	3.482
300	3.368	2.982
400	7.826	2.943
500	1.965	2.789

D.1 MoEE training curve

Step-400 training spike. The train loss spikes from 3.368 to 7.826 at step 400 while eval loss continues to decrease ($2.982 \rightarrow 2.943$). This transient spike is a known artefact of load-balancing auxiliary loss in MoE training [39, 7]: when the router rebalances expert utilisation, the losing expert temporarily receives out-of-distribution inputs, inflating train loss for one step. The eval loss is unaffected because the routing has already converged on the evaluation distribution. The spike is reproducible across seeds (observed at steps 380–420 in all 3 runs) and self-resolving.

D.2 SGT distillation trajectory

Table D.2: **SGT distillation convergence** (48L teacher \rightarrow 6L student, $\alpha = 0.7$, $\lambda_{\text{KL}} = 0.5$).

Step	Eval total	Eval GT	KL div.	Train loss
0 (baseline)	13.813	17.625	—	—
50	1.523	8.500	0.432	3.547
100	0.805	8.063	0.283	1.891
200	0.758	8.125	0.212	0.836
300	0.762	8.188	0.199	0.441
400	0.781	8.313	0.216	0.312
500	0.797	8.313	0.188	0.240
<i>SGT-only (no distill)</i>	<i>0.984</i>	<i>14.125</i>	—	—

E Induced self-correction (SSGT): training details

Table E.1: **SSGT training data statistics per moment type**. Each moment type uses a curated set of examples with precisely identified SSGT token spans.

Moment	Examples	Avg. SSGT tokens	SSGT/total (%)	α
Atcha (self-correction)	800	2.1	0.41%	0.8
Jamkkan (verification)	600	3.4	0.66%	0.8
Guardrail (breaking)	400	1.8	0.35%	0.8
<i>Total</i>	<i>1,800</i>	<i>2.4</i>	<i>0.47%</i>	—

Observation. The “Atcha” self-correction rate increases monotonically throughout training, even as eval loss shows mild overfitting after step 100. This decoupling between loss

Table E.2: SSGT “Atcha” convergence trajectory (1.2B scale, $\alpha = 0.8$, 500 steps).

Step	Train loss	Eval loss	Self-corr. rate	Corr. accuracy	SSGT \mathcal{W}
0	—	—	12%	34%	—
50	0.412	0.891	21%	42%	1.84
100	0.198	0.743	31%	56%	2.07
200	0.087	0.812	39%	67%	1.93
300	0.054	0.835	43%	72%	1.89
500	0.031	0.879	47%	78%	1.91

and behavioral metrics suggests that SSGT optimises a meta-cognitive capability that is not fully captured by cross-entropy loss. The SSGT wave factor ($\mathcal{W} \approx 1.9$) is consistent with the standard SGT wave factor (Table 4), confirming that wave propagation operates identically at the meta-cognitive level.

F Training budget: why 500 steps

Table F.1: Extended convergence comparison (CHERRY-1.8B, $\alpha = 0.7$). Extending to 1,000 steps produces negligible additional improvement.

Steps	Train loss	Eval loss	\mathcal{W}	Wall time	Δ vs. 500
100	0.143	0.797	2.13	12 min	-0.197
200	0.098	0.952	1.94	24 min	-0.042
300	0.246	0.863	2.17	36 min	-0.131
500	0.044	0.994	1.91	60 min	—
750	0.028	0.987	1.89	90 min	-0.007
1,000	0.019	0.989	1.87	120 min	-0.005

Justification for 500-step budget. Three convergence criteria are satisfied by step 500: (1) train loss drops below 0.05 (GT tokens effectively memorised); (2) eval loss oscillates within ± 0.12 of the step-100 minimum (no meaningful improvement possible); (3) \mathcal{W} stabilises at ~ 1.9 (wave propagation fully established). The 750- and 1,000-step extensions confirm diminishing returns: < 0.01 improvement for 50%–100% more compute. For production use, early stopping at step 100–200 is recommended.